Effects of Wood Rays on the Shrinkage of Wood during the Drying Process

Qianwen Xue,[a] Weisheng Sun,[a,b,*] Kurt Fagerstedt,[c] Xi Guo,[a,b] Mingrui Dong,[a] Wenbin Wang,[a] and Huimin Cao [a]

To elucidate the origin of shrinkage anisotropy of wood during the drying process, wood from three tree species, *Quercus* sp., *Juglans nigra*, and *Pometia pinnata*, was analyzed using thin cryomicrotome sections and sequential drying on a micro-scale. The data on shrinkage, based on the transverse direction, were calculated using Image Pro Plus software to measure the thickness of the cell wall of fibers. The results showed that: (1) In the tangential direction, the shrinkage of wood fibers were all in the "smallest-bigger-smaller (-bigger-smaller)" pattern from A to C (A: The cells closest to the wood rays; C: The cells in the middle between the wood rays) and fibers next to the rays always have the minimum shrinkage at different moisture contents; (2) the width of the rays has no negative correlation with the shrinkage of wood fibers; and (3) the rays have the same effect on the shrinkage of wood fiber cells in both latewood and earlywood. In addition, the shrinkage of latewood is more severe than that of earlywood, which leads to tangential shrinkage.

Keywords: Shrinkage; Wood ray; Restraint; Anisotropy; Drying

*Contact information: a: School of Engineering, Zhejiang A&F University, Lin'an 311300, China; b: Laboratory of Wood Science and Technology, Zhejiang A&F University, Lin'an 311300, China; c: Viikki Plant Science Centre VIPS, Faculty of Biological and Environmental Sciences, University of Helsinki, Helsinki 00014, Finland; *Corresponding author: 18268158266@163.com*

INTRODUCTION

Dimensional stability, mechanical strength, and fire and rot resistance are all very important properties for wood when used in architecture, in interior decoration, and as furniture material. Among these, dimensional stability is the foundation and is greatly dependent on the quality of wood drying. Because wood is an irregular, heterogeneous, and anisotropic material (Thuvander *et al.* 2002), the longitudinal, tangential, and radial shrinkages of wood are different during the drying process, and they may produce drying defects such as cracks, warps, and splits.

Previous reports have clarified that in normal wood, the longitudinal shrinkage from the green to the dried condition is the smallest, while the transverse shrinkage has distinctly higher values. In addition, significant anisotropy has been verified and is manifested in the fact that tangential shrinkage is usually 1.5 to 2.5 times that of radial shrinkage (Spear and Walker 2006). Therefore, understanding the cause of anisotropic shrinkage of wood during the drying process is important for ensuring the dimensional stability of wood.

Many researchers have presented theories related to the anisotropic shrinkage of wood. Panshin and Zeeuw (1980) held the opinion that wood shrinkage happens only when moisture content is below the fiber saturation point (except for certain abnormal cases). Pambou *et al.* (2017) considered that wood is in elastic deformation when the moisture

content is higher than the fiber saturation point while the plastic deformation of wood can not be recovered when the moisture content is lower than the fiber saturation point. In addition, Bonarski *et al.* (2015) considered that wood shrinkage is governed by its chemical composition, ultrastructure, and gross anatomy, and indicated that the transverse shrinkage of wood depends mostly on a specific ultrastructural arrangement of the moderately organized cell wall compounds. Therefore, studying the ultrastructures of wood is one of important ways to understand the shrinkage deeply to ensure the dimensional stability of wood.

There are many theories concerning the ultrastructures that influence the anisotropy behaviors of wood. All factors leading to anisotropic shrinkage of wood on the micro-scale can be divided into three groups: (1) the rays exert a restraining influence on the radial shrinkage of the fibers (Wijesinghe 1959); (2) the transverse shrinkage anisotropy of earlywood is more pronounced than that of the latewood, which increases the tangential shrinkage (Skaar 1988; Pentoney 1953); and (3) the microfibril angle in the S2 layer is an important factor affecting the degree of shrinking anisotropy of wood during the drying progress (Meylan 1968, 1972; Cave 1972; Barrett *et al.* 1972; Koponen *et al.* 1989; Watanabe and Norimoto 1996).

Skaar (1988) believed that both the ray restraint theory and latewood domination theory are most probable in explaining the anisotropy of wood during drying. When it came to latewood domination theory, Gu *et al.* (2001) observed, similarly, that the radial cell wall of Scots pine latewood is about 25% thicker than the tangential wall, while earlywood radial cell walls do not show such a difference. Dang *et al.* (2018) believed that the mean radial strain in latewood is higher than that reached in earlywood during tangential adsorption and tangential desorption. In the ray restraint theory, it is partly believed that rays play the most important role in restraining radial shrinkage, as the ray tissue shrinks less in the radial direction. However, Boutelje (1962) denied the importance of rays in this regard in some species. Wu *et al.* (2006) presented that ray parenchyma proportions determine total shrinkages. Taylor *et al.* (2013) reported that the shrinkages near the rays are smaller than the shrinkages distant from the rays by employing X-ray computed tomography, which directly confirms the "ray-restraint" on the micro-scale. Patera *et al.* (2018) revealed that the role of rays in the cellular structure in restraining the tangential swelling of thin-cell-walled earlywood.

The literature about ray restraint theory mentioned above were based on the research of effect of wood rays on a region of wood fibers, which considered total shrinkages rather than unit shrinkage. Therefore, in the view of the authors, there are good reasons to assume that rays also are responsible for the effect on unit shrinkage of wood fibers in this context.

To enrich the explanation of the inhibitory effect theory of xylem rays on radial shrinkage and to clarify how the structures affect shrinking of earlywood and latewood during the drying process, an experiment to observe the shrinkage of wood fiber cells between two wood rays was designed. The experiment also compared the difference between earlywood and latewood using thin cryomicrotome sections and Image Pro Plus to find a region of interest (ROI) to measure the thickness of the cell wall of fibers during sequential drying.

EXPERIMENTAL

Specimens

Three types of woods from Zhejiang Province in China were selected: ring porous wood (oak; *Quercus* sp.), semi ring porous wood (black walnut; *Juglans nigra*), and diffuse porous wood (pometia; *Pometia pinnata*). Every block was selected from mature tree sapwood with dimensions of 20 × 20 × 20 mm, cut with the use of a wheel saw. All wood blocks were soaked in distilled water for 5 days and then divided into four parts with dimensions of 10 × 10 × 10 mm. Finally, 25 µm sections were cut with a cryomicrotome at -12 ºC and placed in a dish with distilled water.

For measurements, one glass slide, one cover slip, and two pieces of tape were weighed in grams (w_n, n = number of samples). Three pieces of wood sections were selected and placed on the slide together for precise weighing. The sections were covered with the cover slip and taped down. The slides were marked with the first letter of the wood species and number (*e.g.*, J01, Q01, P01). No glue or other media that could possibly interfere with the wood samples were used during drying.

Classification of Wood Fiber Cells

In order to observe the ray restraint theory, the xylem cells were classified into three categories: A, B, and C, as shown in Fig. 1.

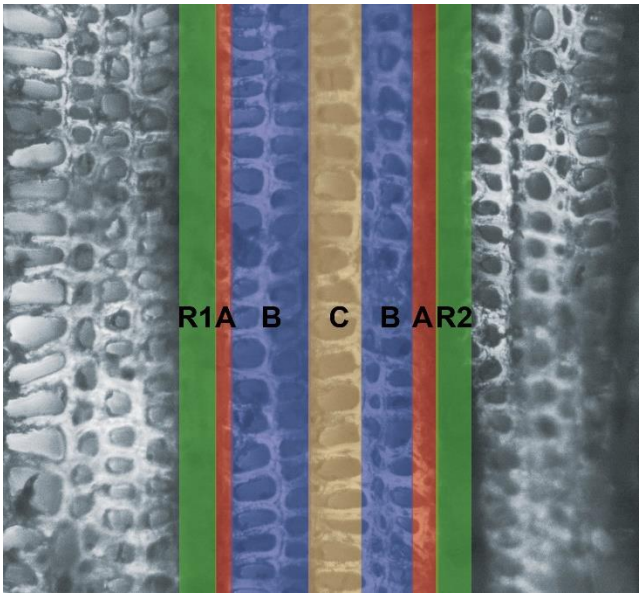

Fig. 1. The classification of cells for measurements in a cross section (take *Pometia pinnata* as an example). A: The cells closest to the wood rays; B: The cells close to A and between the wood rays (the smaller the number is, the closer it is to the rays); C: The cells in the middle between the two rays; R1: The rays on the left of the picture; R2: The rays on the right of the picture.

Measurement of the Shrinking Process

The specimen was dried gradually in a drying oven at 105 ºC. The weight in grams W_{na} (n = number of sample; a = 0, 15, 30 min, the period of drying) and the cell wall thickness D (µm) of the specimens were recorded every 15 min. Image Pro Plus (IPP) 6.0 software (Media Cybernetics, Rockville, USA) designed for cell measurements was used

to measure the cell wall thickness. As is shown in Fig. 2, IPP was used to find a region of interest (ROI) according to color (a1) to generate the contours of the wood fibers (a2). The area of the cell wall was measured automatically by IPP through find ROI (white in a2). Then, the skeleton of the cells were generated by the "thinning function" of IPP. Also, they were measured automatically by IPP.

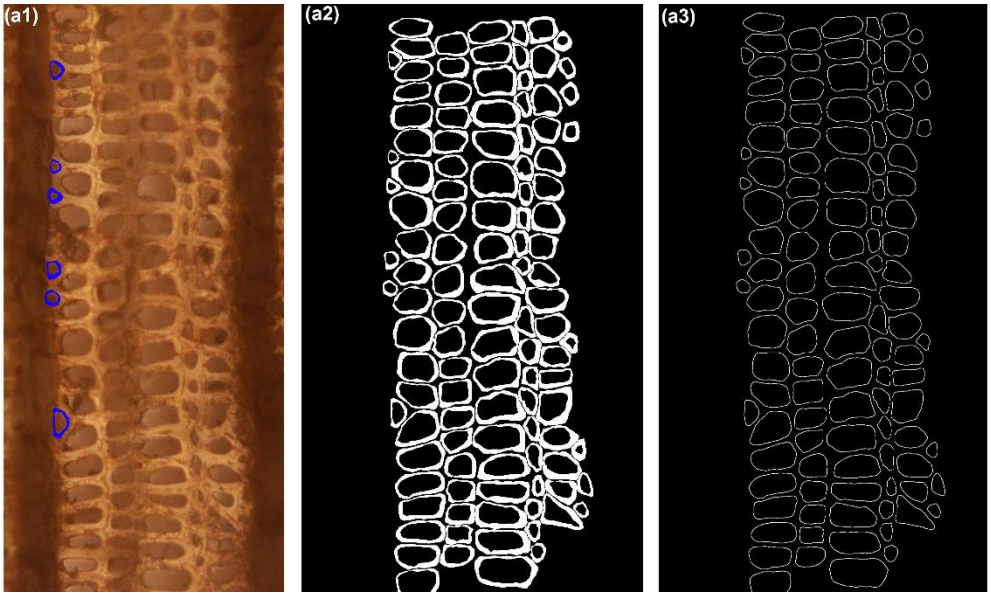

Fig. 2. The image processing used to elucidate the method of cell wall measurement from anatomical image of wood. Take *Pometia pinnata* as an example, a1: original unprocessed image; a2: the contours of the wood fibers; a3: the skeleton of the wood fibers.

As described in Liu and Zhao (2012), the absolute moisture content of the specimens (J01, J02, J03, Q01, Q02, Q03, P01, P02, P03), M (%), at every drying step, was calculated with Eq. 1,

$$\mathrm{M} = \frac{(W_{00} - w) - (W - w)}{W - w} \times 100(\%) \quad (1)$$

where W_{00} is the weight of samples in the green condition, W *is* the weight at the particular moisture content, and w is the total weight of samples except of slices including one glass slide, one cover slip, and two pieces of tape.

As described in Redman *et al.* (2016), the average cell wall thickness in different directions, D (μm), was calculated using Eq. 2,

$$D = S/C \quad (2)$$

where S (μm^2) is the area of the cell wall (Fig. 2, a2) and C (μm) is the perimeter of the cell wall (Fig. 2, a3).

As described in Redman *et al.* (2016), the average fiber liner shrinkage of every column, y, was calculated with Eq. 3,

$$\mathrm{y} = \frac{\sum_{n=1}^{n} \frac{D_{00} - D}{D_{00}} \times 100(\%)}{n} \quad (3)$$

where n (more than 50 cell walls) is the number of the cell walls, D_{00} (μm) is the cell wall thickness in the green condition, and D *(μm)* is the cell wall thickness at the particular moisture content.

RESULTS AND DISCUSSION

The Effect of Position on the Shrinkage of Wood Fibers between Two Rays

Figure 3 shows the effect of rays on the shrinkage of wood fiber cells between two rays at different moisture contents, and the specific parameters are shown in Table 1 and Table 2. Latewood and earlywood from each species were analyzed. No matter latewood or earlywood from each species, the shrinkage of wood fibers under the fiber saturation point (FSP), above the FSP, or even at the saturation situation was all presented the similar regulation in Fig. 3. From A to C, the shrinkage of wood fibers always was in the "smallest-bigger-smaller (-bigger-smaller)" pattern. What is more, the difference between the peak and valley in this pattern increased with the decrease of the moisture content.

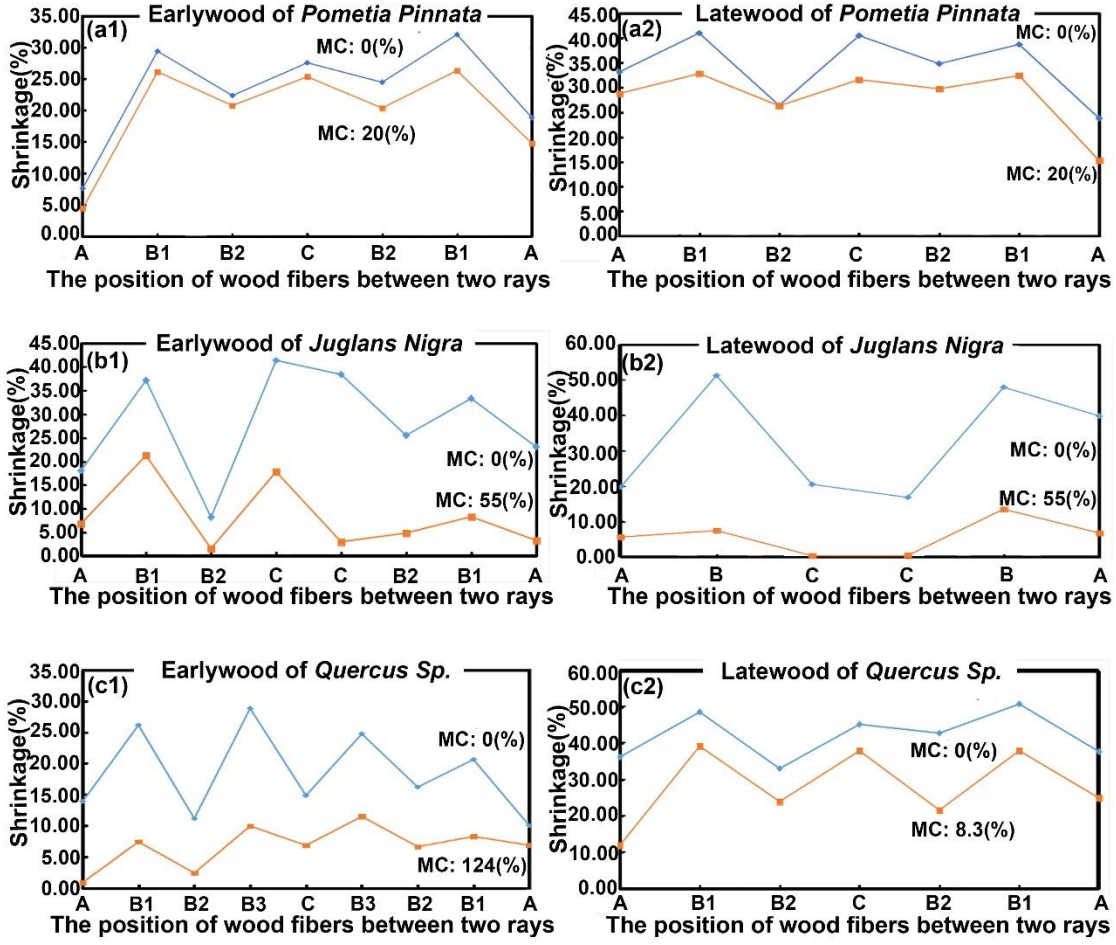

Fig. 3. The effect of rays on the shrinkage of wood fiber cells between two wood rays. The shrinkage behavior of latewood and earlywood of *Pometia pinnata* between two wood rays is plotted in (a1, a2), respectively, while in (b1, b2) that of *Juglans nigra* is showed. (c1, c2) describes the shrinkage behavior of latewood and earlywood *Quercus sp*.

In Table 1, wood fibers in the A position had the minimum shrinkage except the latewood of *Juglans nigra* and the shrinkage of wood fibers in the B position was greater than that in the A position; however, the shrinkage in the B position was smaller than that in the C position in most cases except in the latewood of *Juglans nigra* and in earlywood of *Quercus sp.* (Table 1.). In addition, the shrinkage of wood fibers in the C position was always changing, sometimes with greater (a1, a2, b1, c2), and sometimes with less shrinkage (b2, c1). Table 2 shows the effects of different rows of wood fibers on wood shrinkage through comparing the shrinkage of fibers in the A, B, and C position and the average shrinkage. The results were that the amount of the shrinkage in the A position was lower than the average shrinkage except the latewood of *Juglans nigra*. However, when compared with average shrinkage, the shrinkage of fibers in the B or C position sometimes was higher, sometimes was lower.

Table 1. The Shrinkage of Fibers between Two Rays (%)

Species	A		B		C	
	EW	*LW*	*EW*	*LW*	*EW*	*LW*
Pometia pinnata	13.2	28.4	27.0	35.2	27.5	40.4
Juglans nigra	20.5	29.8	26.0	49.6	39.9	18.7
Quercus sp.	11.9	37.0	21.3	43.9	14.8	45.3
EW, earlywood; LW, latewood						

Table 2. Effects of Different Rows of Wood Fiber Cells on Wood Shrinkage (%)

	A		B		C	
Species	Average-*EW*	Average-*LW*	Average-*EW*	Average-*LW*	Average-EW	Average-*LW*
Pometia pinnata	9.39	6.26	-4.45	-0.50	-4.94	-5.76
Juglans nigra	8.29	-13.82	2.80	-16.93	-11.09	14.08
Quercus sp.	4.07	5.07	-5.25	-1.84	1.17	-3.24
EW, earlywood; LW, latewood						

On the whole, wood fibers in the A position had the minimum shrinkage because the rays inhibited wood fiber shrinkage. This is consistent with the "ray restraint" theory on the micro-scale in a single sample (Taylor *et al.* 2013). The shrinkage of wood fibers always was in the “smallest-bigger-smaller (-bigger-smaller)” pattern from A to C (Fig. 3.), so it cannot be concluded that more distance from the rays results in a smaller restraint stress or greater wood fiber shrinkage. In the drying progress, the cell wall will shrink when the moisture content is under the FSP; however, according to Fig. 3, the cell wall had already shrunk when the moisture content was above the FSP (b1, b2, c1). Because the cell wall is made up of primary wall, secondary wall, and middle lamella (Fig. 4.) (Liu and Zhao 2012) and bound water is in the primary wall and secondary wall while free water is in the middle lamella, it can be inferred that the middle lamella has already shrunk above the FSP, leading to the shrinkage of the cell wall. Figure 3 (a1, a2, c2) showed that there was a similar regulation as others when the moisture content was under FSP; however, the difference of the peak and the valley was larger than that in b1, b2, c1. Therefore, it can be guessed that not only the middle lamella has the influence on the shrinkage of the fibers, but also the secondary has and even more pronounced.

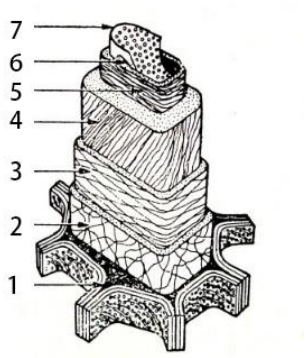

Fig. 4. 1. middle lamella; 2. primary wall; 3. outer layer of secondary wall (S1); 4. middle layer of secondary wall (S2); 5. lining layer of secondary wall (S3); 6. Spiral thickening; 7. wart layer; Reprinted with permission from Liu and Zhao (2012).

Wijesinghe (1959) also made a quantitative study of the shrinkage of fibers while attached to rays in sections and when isolated from them to find out whether the rays restraint stresses are the sole cause of differential shrinkage. When the rays were dissected from the sample, through analyzing the interaction effect between wood rays and a region of the wood fibers, it can be concluded that the radial shrinkage of wood fibers was larger than that in the situation without dissecting from the sample, and the radial shrinkage of rays was less while tangential shrinkage of that was also larger. Therefore, there was a restraint between rays and wood fibers when rays were not dissected out from the samples and vice versa. To some degree, this method had some limitation. It only demonstrated that there was a stress between rays and wood fibers without qualitatively reflecting the specific force of wood rays on wood fiber cells. At the same time, Bosshard (1956) has stressed the importance of the degree of lignifications of the middle lamella as one of the causes of anisotropic shrinkage, which is consistent with the idea in the present manuscript. In brief, the degree of lignification of the middle lamella, the influence of the secondary wall, and ray restraint theory were all used to explain the "smallest-bigger-smaller (-bigger-smaller)" pattern from A to C (Fig. 3.), but further investigation is needed.

The Effect of Ray Width on the Shrinkage of Wood Fibers

Table 3 shows that in earlywood, in the A and B positions of the three different species, wider rays coincided with less fiber shrinkage. However, this conclusion was not always true in the C position. Furthermore, in latewood it was only suitable for the fibers at A position of *Pometia pinnata* and *Juglans nigra*. All the other results in Table 4 are in opposition of the conclusion above; wider rays were observed with more fiber shrinkage. As a result, the width of the rays showed no negative correlation with the shrinkage of wood fibers next to the rays, which is consistent with the conclusion that the rays have a restraining influence on the radial shrinkage of the fibers. However, the difference between species does not appear to bear any relation to their ray size. The effect of the ray width on the radial shrinkage of the wood fiber cells was determined qualitatively by observing the maximum curvature of the sample (Wijesinghe 1959), and the result was similar to that of this manuscript.

In general, fiber shrinkage is clearly dependent on the distance from the wood rays. Fibers in the A position shrink most because wood rays consist of transversely arranged cells, and as such they differ from other wood cells and restrain the radial shrinkage in the process of drying. In addition, the width of the rays has no relationship with the shrinkage

ratio.

Table 3. The Shrinkage of Fibers near Rays in Earlywood (%)

Species	Ray Width (μm)		Fiber Shrinkage in Earlywood (%)					
			A		B		C	
	R1	R2	Next to R1	Next to R2	Near R1	Near R2	Near R1	Near R2
Pometia pinnata	17.5	15.1	7.6	18.8	25.9	28.2	27.5	
Juglans nigra	17.3	14.5	18.0	23.0	22.6	29.4	41.4	38.4
Quercus sp.	8.8	17.3	13.9	9.9	22.0	20.5	14.8	

Table 4. The Shrinkage of Fibers near Rays in Latewood (%)

Species	Ray Width (μm)		Fiber Shrinkage in Latewood (%)					
			A		B		C	
	R1	R2	Next to R1	Next to R2	Near R1	Near R2	Near R1	Near R2
Pometia pinnata	11.2	12.1	33.1	23.7	33.6	36.7	40.4	
Juglans nigra	24.1	8.3	19.8	39.8	51.3	48.0	20.5	16.9
Quercus sp.	10.3	13.5	36.3	37.8	40.9	46.9	45.3	

The Effect of the Latewood and Earlywood on the Shrinkage of Wood Fibers

For the three species, the shrinkage of earlywood and latewood fibers were all in the "smallest-bigger-smaller (-bigger-smaller)" pattern from A to C at different moisture contents, as shown in Fig. 3; however, the shrinkage of earlywood from green to dry was always smaller than that of the latewood, which increased the tangential shrinkage (Table 1). This result was attributed to the different cell wall contents. Specifically, because the earlywood is light and soft, the material content of the cell wall is less and the density is low, and as such the shrinkage of the earlywood is small. Furthermore, because the earlywood and latewood are in parallel, the larger shrinkage of latewood forces the earlywood to dry together, which increases the tangential shrinkage. A similar observation was also made by Watanabe *et al.* (1996).

CONCLUSIONS

1. Two main reasons for wood shrinkage can be reflected in these three different tree species: (1) the shrinkage of the latewood is greater than that of earlywood, which increases tangential shrinkage; (2) the radial shrinkage of wood decreases due to ray restraint.
2. Shrinkage of fibers between two rays always were all in the "smallest-bigger-smaller (-bigger-smaller)" pattern from A to C due to the degree of lignification of the middle lamella, the influence of the secondary wall, and wood ray restraint. Among them, the fibers next to the rays always have the smallest shrinkage, while that of fibers in the

middle of the two rays varies.

3. The width of the ray has no negative correlation with the shrinkage of the fibers next to the rays.

ACKNOWLEDGMENTS

The authors appreciate the financial support from National key research and development plan: "integration and demonstration of valuable tree species floor value-added processing technology" (2017YFD0601105), support of experimental technology from Viikki campus of University of Helsinki.

REFERENCES CITED

Barrett, J. D., Schniewind, A. P., and Taylor, R. L. (1972). "Theoretical shrinkage model for wood cell walls," *Wood Science* 4(3), 178-192.

Bonarski, J. T., Kifetew, G., and Olek, W. (2015). "Effects of cell wall ultrastructure on the transverse shrinkage anisotropy of Scots pine wood," *Holzforschung* 69(4), 501-507. DOI: 10.1515/hf-2014-0075

Bosshard, H. H. (1956). "Über Die Anisotropie der Holzschwindung," *Holz als Roh- und Werkstoff* 14(8), 285-95. DOI: 10.1007/BF02605214

Boutelje, J. (1962). "The relationship of structure to transverse anisotropy in wood with reference to shrinkage and elasticity," *Holzforschung* 16(2), 33-46. DOI: 10.1515/hfsg.1962.16.2.33

Cave, I. D. (1972). "A theory of shrinkage of wood," *Wood Sci. Technol.* 6(4), 284-292. DOI: 10.1007/BF00357050

Dang, D., Moutou, P. R., Toussaint E., and Grédiac M. (2018). "Inverse identification of early- and latewood hydric properties using full-field measurements," *Wood Material Science & Engineering* 13(1), 50-63. DOI: 10.1080/17480272.2016.1263973

Gu, H., Zink-Sharp, A., and Sell, J. (2001). "Hypothesis on the role of cell wall structure in differential transverse shrinkage of wood," *Holz als Roh- und Werkstoff* 59(6), 436-442. DOI: 10.1007/s001070100240

Koponen, S., Toratti, T., and Kanerva, P. (1989). "Modelling longitudinal elastic and shrinkage properties of wood," *Wood Sci. Technol.* 23(1), 55-63. DOI: 10.1007/BF00350607

Liu, Y. X., and Zhao, G. J. (2012). "Wood cells," in: *Wood Science*, China Forestry Publishing House, Beijing.

Meylan, B. A. (1968). "Cause of high longitudinal shrinkage of wood," *For. Prod. J.* 18(4), 75-78.

Meylan, B. A. (1972). "The influence of microfibril angle on the longitudinal shrinkage moisture content relationship," *Wood Sci. Technol*. 6(4), 293-301. DOI: 10.1007/BF00357051

Pambou Nziengui C. F., Ikogou S., and Moutou Pitti R., (2017). "Impact of cyclic compressive loading and moisture content on the mechanical behavior of *Aucoumea klaineana* Pierre," *Wood Material Science & Engineering* 13(4), 190-196. DOI: 10.1080/17480272.2017.1307281

Panshin, A. J. and Zeeuw, C. D. (1980). "Structure," in: *Textbook of Wood Technology*, McGraw-Hill, New York.

Patera, A., Bulcke, J. V. D., Boone, M. N., Derome, D., and Carmeliet, J. (2018). "Swelling interactions of earlywood and latewood across a growth ring: Global and local deformations," *Wood Sci. Technol.* 52(7), 91-114. DOI: 10.1007/s00226-017-0960-3

Pentoney RE. (1953). "Mechanisms affecting tangential *vs.* Radial shrinkage," *For. Prod. J.* 3(2), 27-32.

Skaar, C. (1988). "Hygroexpansion in Wood," in: *Wood-Water Relations*, Springer Series in Wood Science, Springer, Berlin, Heidelberg. DOI: 10.1007/978-3-642-73683-4_4

Spear, M., and Walker, J. (2006). "Dimensional instability in timber," in: *Primary Wood Processing, Principles and Practice*, Springer, Berlin. DOI:10.1007/1-4020-4393-7_4

Taylor, A., Plank, B., Standfest, G., and Petutschnigg, A. (2013). "Beech wood shrinkage observed at the microscale by a time series of X-ray computed tomographs (μXCT)," *Holzforschung* 67(2), 201-205. DOI: 10.1515/hf-2012-0100

Thuvander, F., Kifetew, G., and Berglund, L. A. (2002). "Modeling of cell wall drying stresses in wood," *Wood Sci. Technol.* 36(3), 241-254. DOI: 10.1007/s00226-001-0134-0

Watanabe, U. and Norimoto, M. (1996). "Shrinkage and elasticity of normal and compression wood in conifers," *J. Japan Wood Res. Soc.* 42(7), 651-658.

Wijesinghe, L. C. A. D. S. (1959). "The shrinkage of rays and fibres in wood," *Forestry* 32(1), 31-38. DOI: 10.1093/forestry/32.1.31

Wu, Y. Q., Hayashi, K., Liu, Y., Cai, Y., and Sugimori, M. (2006). "Relationships of anatomical characteristics versus shrinkage and collapse properties in plantation-grown eucalypt wood from China," *J. Wood Sci.* 52(3), 187-194. DOI: 10.1007/s10086-005-0751-6

Article submitted: May 11, 2018; Peer review completed: June 15, 2018; Revised version received: July 17, 2018; Accepted: July 23, 2018; Published: August 1, 2018.
DOI: 10.15376/biores.13.3.7086-7095